Structure and Chain Conformation in Poly(methyl-*n*-alkyl)silanes

W. Chunwachirasiri, I. Kanaglekar, and M. J. Winokur*

Department of Physics, University of Wisconsin, Madison, Wisconsin 53706

J. C. Koe† and R. West

Organosilicon Research Center, Department of Chemistry, University of Wisconsin, Madison, Wisconsin 53706

Received April 2, 2001; Revised Manuscript Received June 25, 2001

ABSTRACT: Three asymmetrically substituted methyl-alkyl-substituted polysilanes, poly(methyl-*n*-propyl)silane, poly(methyl-*n*-butyl)silane, and poly(methyl-*n*-hexyl)silane, have been studied using conventional X-ray ray diffraction and direct measurements of the local structure (through a pair correlation function analysis) in combination with UV absorption spectroscopy. These data universally support Si backbone models which are dominated by the presence of mixed transoid (T), deviant (D), and, possibly, ortho (O) conformations with dihedral angles approximating ±170°, ±155°, and ±90°, respectively. There is no evidence for a significant fraction of all-anti (A, i.e., trans-planar), all-transoid, or anti-gauche conformers. Crystalline poly(methyl-*n*-hexyl)silane incorporates a D/T-based Si backbone, and this, locally, approximates a D+T+D−T− motif. Poly(methyl-*n*-hexyl)silane displays a number of low-temperature polymorphic structures, and one of these is found to exhibit Bragg-like scattering features. Temperature-dependent UV absorption measurements of poly(methyl-*n*-hexyl)silane resolve two distinguishable isosbestic points and are indicative of mesomorphic behavior.

Introduction

Organopolysilanes comprise a diverse family of electroactive polymers[1−4] in which delocalization of the bonded Si σ electrons (i.e., σ conjugation) leads to a strong absorption band in the ultraviolet (UV) spectral region in close analogy to that of the lower energy $\pi-\pi^*$ transition of π-conjugated polymers. The specific attributes of these interband absorptions are, to first order, correlated with the explicit conformation of the all-Si main chain and, to a lesser extent, the explicit choice of side chain constituent. Formulating the Si-based polymers, nominally as ($[-SiRR'-]_n$), with alkyl-, alkoxy-, or aryl-based side chain substituents leads to materials well-known[5,6] for their pronounced thermochromic response in both solution and the solid state. This thermochromism is intimately related to variations in both the polymer chain conformations and interchain packing. In the simplest case higher temperature is associated with a more disordered phase, shorter effective conjugation length, and a higher energy interband transition while lower temperature correlates with a more ordered phase having an increased effective conjugation length and a lower energy transition. Theoretical studies assuming a simple order−disorder transition (ODT) by Schweizer[7,8] have identified three distinct pathways by which this transition may occur in solution. However, in both the solution and the solid state, the thermochromism can be far more complex,[4,9−11] and the full range of structure/property relationships has yet to be elucidated.

The better known (and far more heavily studied) symmetrically substituted polysilanes (i.e., $-[Si\ R_2]_n-$ where R is an *n*-alkyl chain) exhibit structures and structural phase behavior having a remarkable sensitivity to side chain length, sample temperature, and thermal history. The most compact systems, ranging from poly(dimethylsilane) to poly(di-*n*-hexylsilane), adopt ordered, crystalline phases[12,13] historically identified with either an all-anti (nominally trans-planar) or 7/3 helical[14,15] backbone conformations. These two distinct forms are associated with different $\sigma-\sigma^*$ interband absorption energies.[16,17] When in the helical form, the UV adsorption spectrum is typically peaked near 315 nm (4.0 eV), while the more planar conformation is typically centered at 375 nm (3.3 eV). Poly(dialkylsilane)s with longer alkyl substituents have been cited[17] as having a four monomer AGAG′ repeat and a claimed *intermediate* UV absorption spectrum peaked near 335 nm (3.7 eV).

While the existence of at least two of these limiting forms (anti and helical) is fairly well established, additional studies[18] suggest that the actual situation may be far more complicated and potentially more interesting. An earlier force field modeling study[19] of poly(dimethylsilane) indicated that Si−Si−Si−Si torsion angles of 165° may be energetically favorable. For poly(di-*n*-hexylsilane), in the absence of three-dimensional packing constraints, various anti-gauche conformations (e.g., A_3GA_3G') are claimed to be equally viable main chain structures.[13] Recent studies of silane oligomers are also intriguing. Michl and co-workers[20,21] have found a complex topology of intermediate energy minimum in the available Si backbone conformations with the appearance of ortho (O) and deviant (D) conformations (with nominal dihedral angles of 90° and 155°, respectively) in combination with a splitting of the planar trans to a transoid (T at 170°) form. Clearly the existence of a helical conformation is consistent with an all D^+ or D^- construction. As noted before, there are also the more recent accounts documenting the presence of unusual structural forms and complicated thermochromic transitions in the symmetrically alkyl-substituted polysilanes and in aryl-substituted systems containing chiral moieties.

* Corresponding author: E-mail mwinokur@facstaff.wisc.edu.
† Current address: Department of Chemistry, International Christian University, Osawa, Mitaka, Tokyo 181-8585, Japan.

10.1021/ma0105688 CCC: $20.00
Published on Web 08/16/2001

Comparable studies (though far fewer) of the highly asymmetric methyl-*n*-alkyl systems have also revealed an interesting progression with increasing alkyl chain length. Although atactic, poly(methyl-*n*-propylsilane), pMePrSi, exhibits a significant fraction of partially crystalline material which, when pulled into a fibers, contains a relatively high degree of chain orientation.[22] Analysis of this crystalline fraction is universally claimed to be consistent with a nearly planar chain conformation[22−24] although no corresponding references to the UV absorption properties are made. A UV absorption study of various longer poly(methyl-*n*-alkylsilane)s, by Yuan and West,[25] is indicative of less planar conformations ($\lambda_{max} < 350$ nm). Nearly all of the measured low-temperature UV absorption spectra are peaked at wavelengths close to that of the helical form. Moreover, there is a continuous thermochromic change in the case of poly(methyl-*n*-butylsilane) (pMeBuSi) but, with increasing alkyl chain length, the thermochromism becomes more abrupt. This latter result is the hallmark signature of a "two"-phase model in which there are distinctly different conformational forms at low and high temperature. This crossover can be interpreted using Schweizer's polarizable media theory[7,8] because of the presumed amorphous nature of the polymer family at low temperatures [pMePrSi and poly(ethyl-*n*-propylsilane) excepted].

Since these asymmetric poly(dialkylsilane)s exhibit UV absorption features at wavelengths intermediate to the documented helical or all-trans values, it is also of fundamental interest to clarify whether these features signify the presence of discrete, intermediate conformational forms and whether alternatives to the AGAG′ repeat can be proposed. Although employing a series of atactic asymmetric methyl-*n*-alkylpolysilanes necessarily complicates the situation, the monomer core structural unit, $-CH_2SiCH_3-$, can be viewed from the perspective of local structure as a less complicated starting point for further investigation. In this situation one only need consider the conformations of the structural core and a single alkyl chain fragment per monomer repeat unit.

This report expands the scope of these previous efforts and demonstrates that the complex polymorphism that exists in many of the symmetrically substituted dialkylsilanes also appears in these highly asymmetric systems as well. Slow cooling and rapid cooling (quenching) of poly(methyl-*n*-hexylsilane), pMeHeSi, yields a number of distinctly different structural forms. Motivated by the recent claim[26] for intermediate backbone conformations (i.e., neither all A nor all D) we have reinvestigated the structural refinements of oriented pMePrSi fiber data and obtain clear evidence for the existence of a *local* T+D+T−D− backbone construction. This motif is then used to interpret and justify the local single-chain structure in unoriented films of pMePrSi, pMeBuSi, and pMeHeSi at room temperature (and at reduced temperature) through a pair-distribution-function analysis (PDF) of X-ray scattering data. These PDF analyses suggest that all these polymers, especially at low temperature, have conformations qualitatively consistent with a preponderance of mixed D/T type arrangements.

Experiment Details

All asymmetric polysilanes were synthesized from the corresponding dichlorosilanes by dehalogenative coupling reaction with sodium under standard conditions for polysilane synthesis by Wurtz coupling.[27] High molecular weight fractions (e.g., pMePrSi, $M_w = 15\,000$) were obtained and purified by repeated precipitation from toluene using 2-propanol and methanol. The polymer was dried by heating at 65 °C in vacuo for 72 h. Unoriented films of pMePrSi yielded X-ray profiles similar to those of previous reports.[28] Oriented fibers of pMePrSi were prepared by pulling from a bulk sample at temperatures close to the melting transition (ca. 46 °C) at a rate of approximately 10 cm/s.

X-ray scattering studies were performed on either one of two available diffractometers using a 15 kW rotating anode X-ray generator (Cu $\lambda_{K\alpha} = 1.542$ Å). The first diffractometer employed a focusing bent graphite monochromator and a linear diode array (EG&G model XR1412) detector. The second diffractometer used an elastically bent LiF crystal and a 120° 2θ position-sensitive detector (Inel model CPS-120). Both systems were equipped with full He gas beam paths to minimize absorption and air scatter.

Conventional powder diffraction studies utilized a custom Peltier-based heating/cooling stage (200 to −40 °C) suitably modified by addition of an inlet, which, when necessary, directed a pressurized jet of CO_2 powder onto samples similar to those used in the PDF studies (see below). The existing design achieved cooling rates in excess of 50 °C/s. This in situ quenching chamber was isolated by a pair of thin Be windows.

For the pMePrSi fiber study ($\lambda = 1.542$ Å) a series of radial $\theta-2\theta$ scans were performed using a bobbin of the oriented fibers mounted within a Eulerian cradle. By repositioning these samples, both the equatorial and nonequatorial scattering could be acquired. For the nonequatorial scattering data, the sample was maintained in a symmetrical transmission geometry, and the *c*-axis (or chain axis) orientation was adjusted with respect to the scattering plane of the detector. For comparisons with the structure factor (SF) refinement the data originating from specific layer lines was merged and plotted with respect to the detector angle 2θ. The SF calculations employed a customized link-atom-least-squares (LALS) Rietveld refinement scheme described previously.[29] To qualitatively represent both the syndiotactic (S) and isotactic (I) diads, the basic chain repeat employed an eight monomer segment with a randomly configured sequence of diads invoking a nominal /T+D+T−D−T+D+T−D−/ construction.

PDF analysis is used to assess the local structure, and for polymers, there are specific attributes that are advantageous for resolving the chain conformation. Even in the most crystalline polymers conventional crystallographic refinements often include large Debye−Waller temperature factors, and this is simply indicative of the extensive static and dynamic disorder between polymer chains forming a single crystallite. The net result is that the Bragg scattering peaks are often only resolvable out to 3−4 Å^{-1}, and significantly beyond this point the local structure becomes the dominant contribution. In fact, when appropriately renormalized, the actual impact of the Bragg scattering to the pair correlation function is very modest.[30,31] In less crystalline materials interchain pair correlations usually become even less of an issue.[32] Accessing the scattering out at high wave vector enables a direct measure of the average single chain structure, and in some settings, this information can provide important insight.[33] With respect to the backbone structure, these poly(methyl-*n*-alkylsilane)s are advantageous because the underlying structure base becomes the $-CH_2SiCH_3-$ core with the Si atom providing the dominant contribution. The conformation of the long alkyl side chain has a significantly lesser influence especially in the case of pMePrSi.

Samples used in the PDF study employed 0.6002 Å photons incident on 2 mm thick cylindrical plugs of the unoriented polymer loaded into a thin walled (10 μm thick) glass capillaries. An energy dispersive detector was moved in 0.05 Å^{-1} increments from 0.4 to 20.0 Å^{-1}. The total integrated counts per data point ranged between 3×10^4 and 3×10^5. The raw data were corrected and then converted into two conventional representations, $G(r)$ [or rescaled as $W(r) = r(G(r) - 1)$] and $kS(k)$, where $G(r)$ is a weighted pair-correlation function and

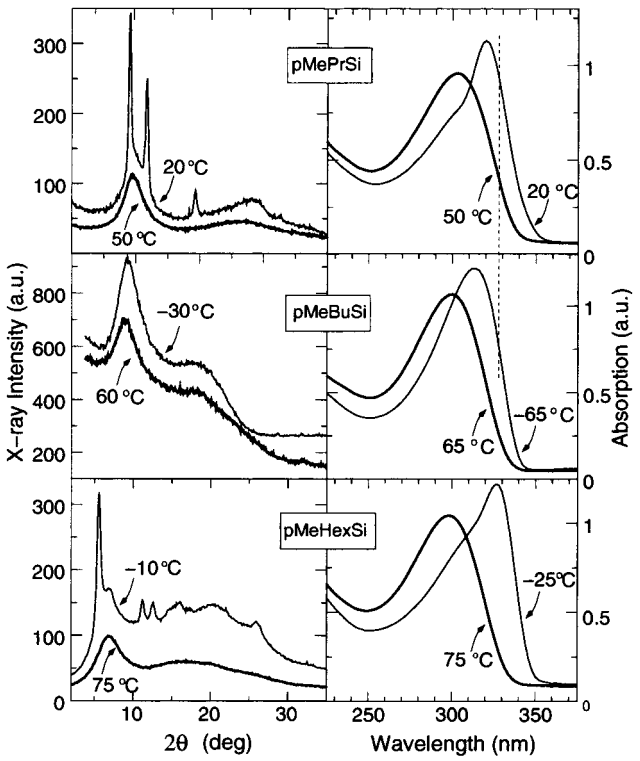

Figure 1. Representative high- and low-temperature X-ray powder diffraction profiles and UV absorption spectra from poly(methyl-*n*-propylsilane), poly(methyl-*n*-butylsilane), and poly(methyl-*n*-hexylsilane). All low-temperature X-ray curves have been rescaled and offset for clarity.

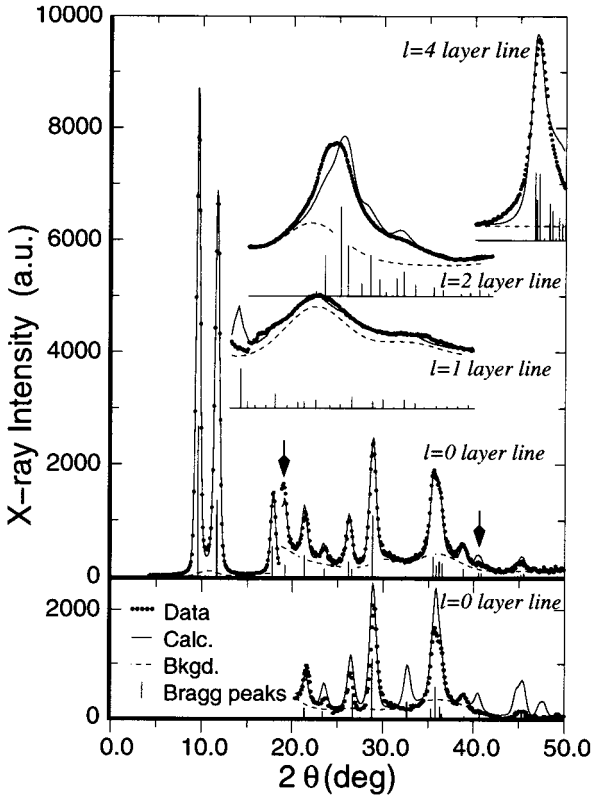

Figure 2. (top) Comparison of pMePrSi fiber data (black dots) with the best-fit curve (thin solid line) using the T+D+T−D− model as described in the text for the $l = 0$, 1, 2, and 4 layer lines ($l \neq 0$ curves are offset). The vertical bars are the underlying Bragg intensities. (bottom) Comparison of pMePrSi fiber data with an original best-fit curve (thin solid line) using a model with a nearly planar backbone conformation (from ref 22).

$kS(k)$ is the k-weighted structure function. In the case of MePrSi, the experimentally derived curve was then compared with calculated profiles using a best-fit model (from structural refinement). The starting point for this calculation was the nominal eight monomer T+D+T−D−T+D+T−D− construction obtained in the conventional powder refinement (and invoking periodic boundary conditions). A fuller account of this methodology is given in ref 31. In general, all eight Si backbone bond angles and dihedral angles were allow to relax subject to simple hard core packing constraints. The C−C−C bond angle was adjustable but treated uniformly while all side chain dihedral angles were also free to relax.

UV absorption spectra were recorded using a Hewlett-Packard HP8452A diode array UV spectrophotometer. Spectra at various temperatures were obtained from polysilane films deposited on thin quartz microscope coverslips. The general procedure was to first cast films from dilute toluene solution and then wait over 12 h before scanning. The same basic CO_2 spray methodology was used to thermally quench the ~2 μm cast films. All UV absorption studies performed in the quenching cell also required two additional quartz windows.

General Results and Discussion of Poly(methyl-*n*-propyl)silane

Example "high" and "low" temperature (with respect to the thermochromic transitions) diffraction and UV absorption spectra for pMePrSi, pMeBuSi, and pMeHexSi are shown in Figure 1, and where available, these data agree with prior reports.[23−25,34,35] PMePrSi clearly undergoes a thermochromic transition, near 45 °C, with improved σ conjugation in the ordered state and a bathochromic shift. The X-ray data also span this order−disorder transition with sharper peaks, indicative of a partial crystallization, forming at temperatures below 45 °C. Jonas et al.[23] analyzed this structure in terms of a two-phase model in which up to 25% of the sample is crystalline, adopting a more trans-like backbone, and the remainder in a less ordered, presumably nematic-like state. With respect to any prior claims of a planar conformation, the UV absorption cannot be reconciled because there are no long wavelength absorption features at or even near 375 nm.[36] Only two (or so) distinguishable components centered about 305 and 320 nm are observed. From this perspective it seems very unlikely that a significant sample fraction adopts an all-transoid or anti conformation.[37] PMeBuSi, as noted by Yuan and West,[25] displays more modest variations in either the UV absorption or X-ray diffraction as a function of temperature. PMeHeSi undergoes a noticeable thermochromic transition with some parallels to pMePrSi. The low-temperature UV absorption again has two components, and these are centered near 310 and 325 nm. The X-ray data clearly support an order−disorder transition with, as seen in the −10 °C scan (obtained after ~1 °C/min cooling), relatively sharp features at 2θ values 5.7° (15.5 Å), 11.4° (7.8 Å), and 12.8° (6.9 Å) suggestive of appreciable interchain ordering. The broader feature, centered about $2\theta = 7.1°$, also narrows at reduced temperature.

PMePrSi is addressed first because it forms oriented fibers and films exhibiting a well-defined equatorial packing, and this structure can be extensively analyzed. Figure 2 presents diffractometer data from a multifiber bundle which has been effectively scanned along each layer line (with l specified by imposing a 7.85 Å chain axis repeat). All sharp features are superimposed upon a slowly varying background which results from scat-

tering by noncrystalline regions and any additional static and dynamic disorder within the crystalline component. The nonequatorial scattering (hkl, $l \neq 0$) exhibits an l-order-dependent smearing along the layer lines; this indicates extensive axial disorder within the crystallites. Still, the overall composite profile (not shown) is similar to those of unoriented samples so it is unlikely that fiber formation induces additional molecular-level structural reorganization.

In unoriented films only the first three intense equatorial reflections are clearly resolved, and the relative intensity ratios of these three peaks can be satisfactorily reproduced using an all-anti[23] (or nearly trans planar[22]) backbone. However, as Figure 2 demonstrates, highly oriented fibers clearly resolve up to additional eight equatorial peaks. Reference 22 has shown that the calculated fit to the equatorial peaks is qualitatively in agreement for many reflections, but quantitative fits are lacking. These systematic failings are reproduced in the bottom most portion of Figure 2 for 2θ angles in excess of 20°. Introducing a nominal T+D+T−D− chain motif, in accordance with the description given in the last section (and the PDF analysis which follows), yields a nearly perfect match between the calculated and experimental ($hk0$) intensities. A few statistically significant discrepancies remain, and these are indicated by vertical arrows. The specific model used here is triclinic (a = 10.18 Å, b = 15.68 Å, c = 7.85 Å, α = 95°, β = 90°, γ = 114°) with two identical chains per unit cell [at fractional positions of (0,0,0) and (0,0.5,0.4)] and average T and D dihedral angles of 7° and 34°, respectively. This staggered two monomer construction shifts the most intense $l = 2$ reflections off-axis and improved the agreement of both the $l = 2$ and 4 layer lines. Because of the extensive axial disordering and the atactic nature of the polymer, the three-dimensional unit cell is not expected to be unique and just approximates a typical structural unit within the crystalline component.

A four monomer, 7.85 Å repeat would be expected to yield evenly spaced layer lines at integer multiples of 0.80 Å^{-1} along the meridional direction. While the calculated $l = 1$ layer line intensity (in Figure 2) is relatively weak, there are no localized scattering features in the experimental data which may attributable to the presence of a clear-cut 7.85 Å repeat. Still, the scattering is strongly dominated by the geometrically constrained $-CH_2SiCH_3-$ core unit, and given the sensitivity of the equatorial data to the explicit chain conformation, it seems likely that something approximating a T+D+T−D− repeat dominates the shortest length scales. In view of the atactic construction of this polymer, it is also unlikely that even more complicated Si backbone repeats are present in large concentrations, for example, T+T+T+D−T−T−T−D+, but these cannot be unequivocally excluded.

Since the claimed structural motif is a local one, PDF analysis provides corroborating evidence. Prior to this discussion, we first motivate and justify our continued use of a simplistic single-chain model. Figure 3 displays selected UV absorption and X-ray diffraction profiles of a pMePrSi sample which was initially quenched from the disordered high temperature phase and then sequentially warmed through the nominal 45 °C ODT temperature. All X-ray spectra, below the thermochromic transition temperature, have profiles consistent with a two-phase coexistence of a minority fraction of

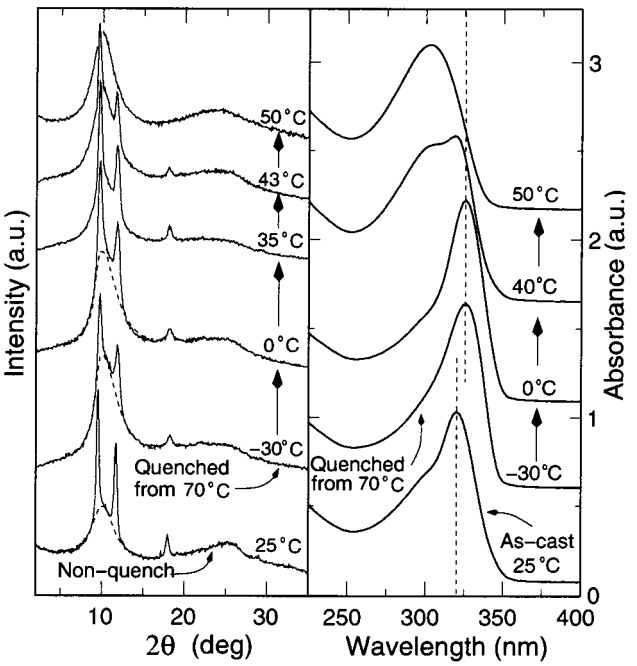

Figure 3. Selected X-ray diffraction and UV absorption spectra from pMePrSi on warming after thermal quenching. Most curves have been offset and scaled slightly for clarity.

the more ordered crystalline phase and majority fraction in a less ordered state. Generally, it is assumed that the long wavelength feature is associated with the more ordered, in this case, crystalline phase. Therefore, it is highly surprising that the relative contributions of the long wavelength (better σ conjugation) and short wavelength (poorer σ conjugation) features in the UV absorption do not exhibit a direct correspondence with the X-ray results. With respect to the nonquenched X-ray profile (and the dashed line), quenching clearly suppresses crystallization and the proportion of polymer associated with this crystallograpically order state. In this example the relative contribution by the crystalline phase is less, and the peaks are noticeably broader. However, the comparable UV absorption profile is peculiar because the $\sigma-\sigma^*$ transition peak is red-shifted 5 nm from that of the as-cast room temperature sample, and this longer wavelength feature has a disproportionately large fraction of the total absorption.

Warming of the quenched sample initially promotes a monotonic increase in the ordered, crystalline scattering albeit with larger peak widths (i.e., a shorter coherence length and/or greater strain) as compared to the nonquenched counterpart. The equivalent UV curve (at 0 °C) exhibits a systematic intensity increase and modest narrowing of the long wavelength feature. Continued warming, to 35 °C and above, now reduces the crystalline fraction and narrows the observed peak widths. Behavior of this type is not unusual in polymers and is often associated with a "melting" by ordered regions within the polymer having the smallest coherence lengths in conjunction with reduced strain. Since there is a rapid increase in the UV absorption at 310 nm and an apparent shift in the long wavelength feature to 320 nm, it seems likely that the largest crystalline domains are actually associated with Si backbone conformations that include intermediate levels of σ conjugation. A reasonable conclusion that can now be drawn is that the same average local chain structure, to a large extent, is present in *both* ordered and

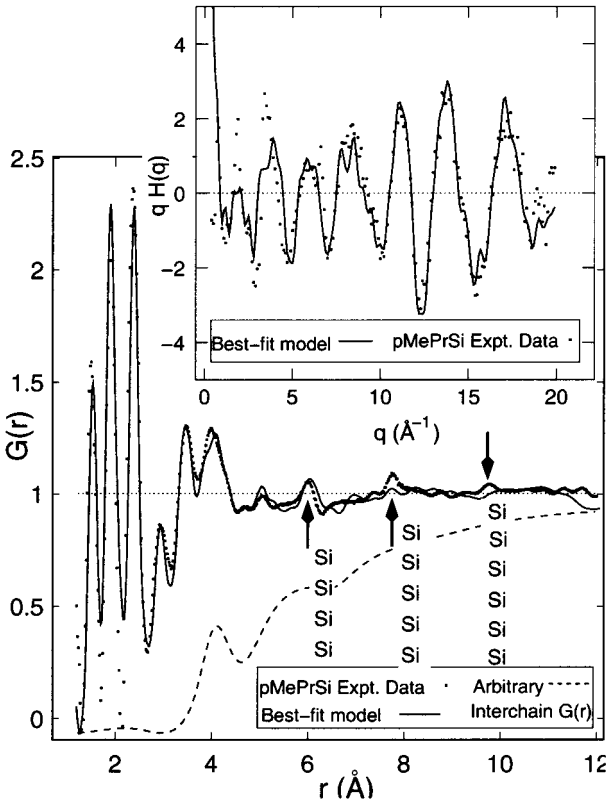

Figure 4. Comparisons between experimental and model derived pair correlation function, $G(r)$, and, in the inset, q-weighted structure function for poly(methyl-*n*-propylsilane). Arrows identify major silicon backbone pair correlations at intermediate distances.

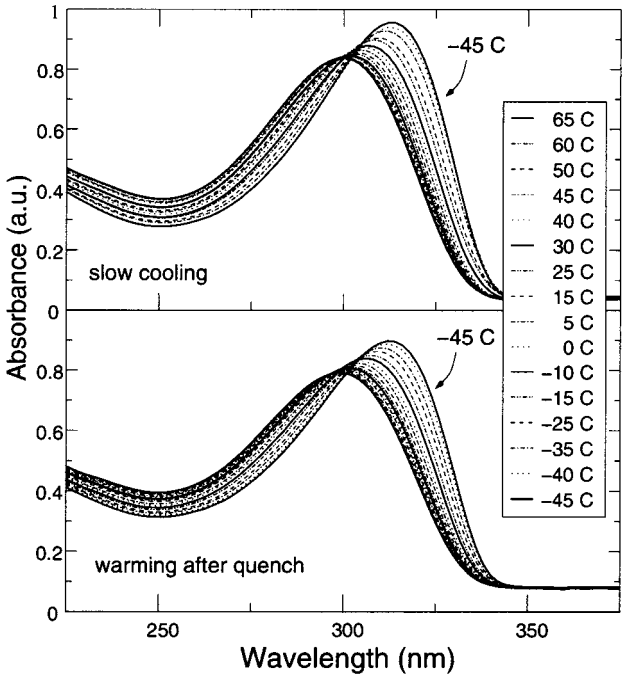

Figure 5. Complete series of UV absorption spectra for pMeBuSi thin film during cooling (top, ~1°C/min) and on warming after thermal quench (bottom).

disordered regions of the polymer. Hence, adopting a simple single-chain model represents a reasonable starting point for assessing the short-range order because it averages over both ordered and disordered regions. A two-phase model might be more appropriate but would also require concomitant increase in the model degrees of freedom.

All X-ray data presented so far have a maximum wave vector of under 2.0 Å^{-1}. The scattering data included in the Figure 4 inset extend out to 20 Å^{-1}, and this region is dominated by scattering from the local single-chain structure. The pMePrSi q-weighted structure function ($qH(q)$, in the inset of Figure 4) best reflects the actual contribution to the pair correlation function $G(r)$. The strongest equatorial reflections, near $2\theta = 10°$ (or 0.7 Å^{-1}), now appear as a single unresolved peak, and they no longer dominate the X-ray scattering profile. Overall, the Bragg scattering, equatorial and nonequatorial, is a minority component with respect to its contribution to $G(r)$. Both curves $qH(q)$ and $G(r)$ really reflect the short-range order averaged over both the ordered and disordered regions of the polymer. The most defining attributes in the experimental $G(r)$ curve are the sharp peaks at 1.52 ± 0.02, 1.91 ± 0.01, and 2.36 ± 0.01 Å corresponding to the C−C, C−Si, and Si−Si bond lengths, respectively. The symmetric dialkylsilane studies of KariKari et al.[13] cite a model that incorporates a 2.41 Å Si−Si bond length; this is clearly not the case in this polymer family. The other key attribute is the persistence of modestly narrow well-resolved peaks centered at 4.00, 5.98, 7.76, and 9.78 Å. These features suggest that, on average, there are local correlations extending out five silicon repeats. Moreover, these results, given an average Si−Si bond distance of 2.36 Å and a Si−Si−Si bond angle of 116 ± 2° (inferred from a 4.00 Å Si−Si−Si spacing), effectively rule out any possibility of nonplanar chain structures with large dihedral torsions such as AGAG′or nearly planar all-T conformations.

Although incomplete, a single-chain model is useful for assessing and analyzing the results at these intermediate length scales. Using the nominal D+T+D−T− motif (as obtained by the Rietveld refinement of the fiber data) as a starting point for the modeling the RDF data, we achieve relatively good agreement in both $G(r)$ and $qH(q)$ in the appropriate regions (i.e., at higher q values), and these results are included in Figure 4 as well. The $qH(q)$ fit improves substantially with increasing q, and this simply reflects the fact that resolvable interchain pair correlations become proportionately weaker at the longer distances. This leads to a more rapid decay in $qH(q)$. A single-chain model clearly does not incorporate interchain correlations. To adequately fit $G(r)$, in which interchain and interchain pair correlations are necessarily superimposed, a slowly varying interchain $G(r)$ background must be arbitrarily imposed.

These results demonstrate, *but do not prove uniquely*, that approximating a D+T+D−T− repeat is fully consistent with the average local structure. Assuming more planar (i.e., all-A or all-T) or AGAG′ constructions does not work well. A highly disordered helical (all-D) model also fits but not quite as well. The specific model depicted in Figure 5 has an average 119° Si−Si−Si bond angle and an average dihedral angle of 158°. The range of dihedral angles are somewhat larger than those of the original starting point (i.e., that of the Rietveld refinement) and therefore reflect the increased disorder of chains presumably residing in the noncrystalline sample fractions. Overall, the most difficult aspect to reconcile with this model was the relative intensity ratios of the three $G(r)$ peaks at 2.96, 3.46, and 4.00 Å. To achieve this effect, Si−Si−Si bond variations in

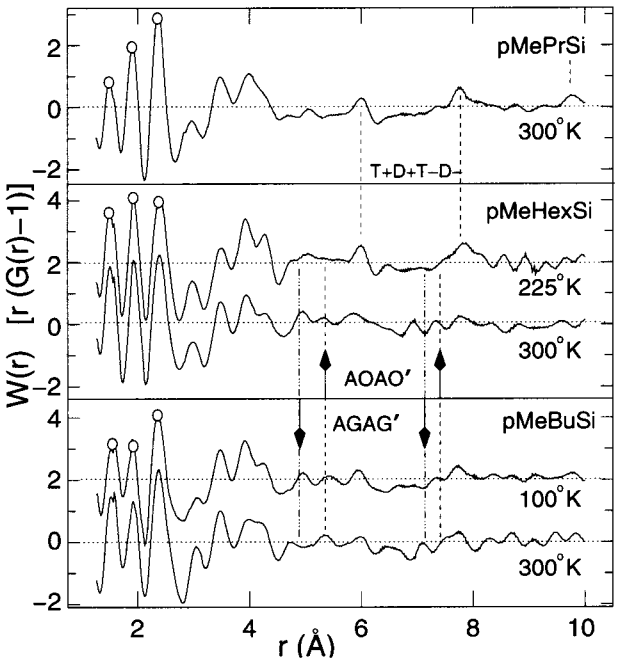

Figure 6. Five representative pair correlation functions, in the form $W(r)$, for the three asymmetrical poly(alkylsilane)s studied: pMePrSi, pMeBuSi, and pMeHexSi.

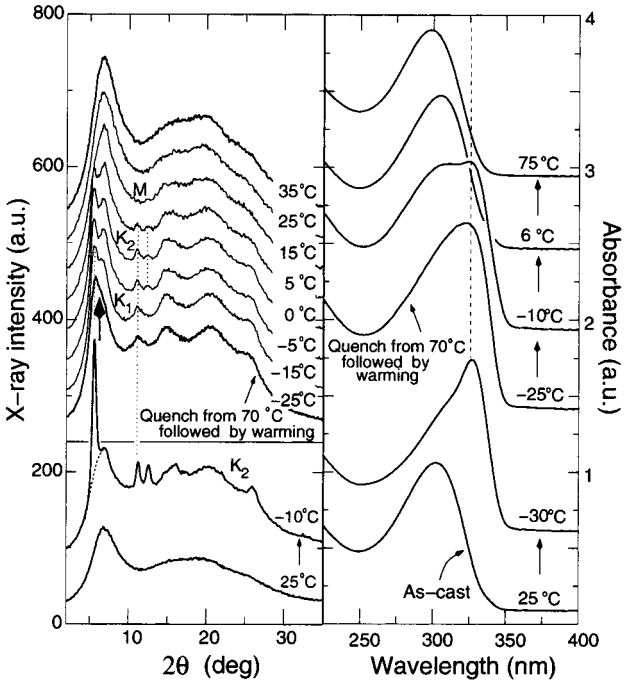

Figure 7. Selected X-ray powder diffraction profiles and UV absorption spectra from pMeHexSi on warming after thermal quenching in conjunction with representative curves from cooled, nonquench samples. Most curves have been slightly rescaled and offset for clarity.

excess of ±10° were necessary. Assuming more uniform Si−Si−Si bond angles gave overly large intensities at the 3.46 Å peak position (which is dominated by nonbonding C−Si pair correlations). A secondary consequence of the large bond angle variation is that the calculated $G(r)$ intensity variations now diminish too quickly with increasing r. We also note that the model coordinates, when examined with an empirical force field such at MM2, includes some unphysically close pair distances.[38] Despite these shortcomings, this single chain model does reflect the underlying backbone conformational order. The major finding is that UV absorption signatures in the vicinity of 325 nm may be associated with structures intermediate to either helical or all-anti conformations. It also seems likely that these results extend to the symmetrical polydialkylsilane family as well.

Discussion of Poly(methyl-*n*-butyl)silane and Poly(methyl-*n*-hexyl)silane

The results for pMeBuSi, as noted earlier, are relatively uneventful and show no evidence of a discrete structural ODT. PMeBuSi is amorphous although cooling, referring back to Figure 1, does sharpen the two broad peaks located near 2θ values of 10° and 25°. Quenching from high temperature also has a minimal effect, and as Figure 5 demonstrates, the UV absorption profiles are almost identical whether on heating (after a quench) or on slow cooling. There is a modest 25 nm blue shift on warming with no evidence of an isosbestic point.

The local pMeBuSi structure, now depicted in the form $W(r)$ where $W(r) = r[G(r) - 1]$, for two representative temperatures is shown in Figure 6, and once again, there are no clear-cut signatures indicative of extensive changes in the local structure. The relative contribution of the 1.53 Å peak increases, in comparison with the PMePrSi data, and this reflects the additional C−C pair correlations due to the increased alkyl chain length. In addition, the three peaks associated with extended Si backbone conformations (previously at 5.98, 7.76, and 9.78 Å) are now less distinctive when compared to the surrounding intensity variations. Overall there are some qualitative similarities[39] of the average chain structure in direct comparison to the pMePrSi data, but distinct quantitative differences are evident, especially in the range 4.5−6.5 Å.

The results for pMeHexSi are far more complex. Figure 6 also includes two representative pair correlation curves at temperatures above and below the thermochromic ODT. The 300 K profile, at intermediate distances, more closely resembles the pMeBuSi data while the low-temperature data, from a sample cooled at approximately 5 °C/min, at 225 K has the same key features contained in the pMePrSi data. The order−disorder transition, and the associated thermochromism, is again strongly correlated with the formation of an intermediate backbone conformation, neither all-anti nor AGAG′, which is dominated by combinations of D and T dihedral conformations.

For pMeHexSi the actual situation is especially subtle. With modest cooling (at approximately 5 °C/min) the polymer exhibits partial crystallization to a "K" phase. This only occurs at temperatures somewhat below 5 °C. Examples curves are shown in Figure 7. Quenching from the high-temperature disordered phase, also shown in Figure 7, fully suppresses formation of this ordered phase. The quenched −25 °C profile contains some vestiges of the ordered structure, but it is dominated in the low angle region by peaks of intermediate width centered at 2θ values of 6.4°, 11.5°, 15.2°, 20.9°, and 27.0°. The corresponding UV absorption profile has just a single, relatively broad feature centered near 320 nm. Stepwise warming resolves a number of distinct processes. There is clear evidence of cold crystallization with, in this case, minimal formation of the ordered phase. The actual proportion of this phase

varies greatly with the specific quench dynamics. Interestingly, the two 2θ peaks near 5.7° and 11.4° evolve and sharpen prior to the formation of the third peak at 12.7°. The first two peaks are simply first- and second-order reflections of a 15.6 Å *d* spacing while the third peak must be associated with a secondary ordering of different crystallographic planes. This complex behavior is comparable to other mesomorphic polymers[40] in which warming from a quenched state allows for sequential formation of closely related crystalline forms. We designate these as K_1 and K_2, and both are metastable. The K phase peaks diminish rapidly upon further warming and are no longer resolvable at temperatures in excess of 10 °C.

The single low-angle 6.4° peak (denoted by an arrow just below the −25 °C X-ray data set) appears to include two superimposed components because, on warming after the quench, it simultaneously evolves into a sharper peak centered about 7.2°. This feature and the broader peak near $2\theta = 15.2°$ arise from a separate structural constituent since only both these features persist to temperatures approaching 20 °C. This form (designated "M"), and not the K phases, is the most thermodynamically stable low-temperature structure. Once formed, the M phase does not, for the most part, revert back to either K phase. A complete account of this process and the full impact of the specific thermal history has not been established. Comparable UV absorption spectra, after a quench, first exhibit a single broad absorption maximum at 315 nm, next two distinguishable maxima (at 305 and 320 nm), and then, by 6 °C, once again a single maximum centered near 305 nm. With continued warming the 305 nm feature reverts to 295 nm. Naively, the 320 nm absorption is associated with the K phases while the 305 nm maximum corresponds to the claimed M phase.

A perfect one-to-one correspondence of the various UV absorption features to specific structural phases is not observed. The cooling UV absorption data shown in Figure 8 are unambiguous in resolving two distinguishable isosbestic points. With respect to this slow cooling data, the first conformational transition is effectively completed by 5 °C while the second one (from 305 to 320 nm) is not clearly resolved until temperatures below −15 °C.

DSC data of ref 25 (at a cooling rate of 20 °C/min) display three endothermic features at temperatures near 0, −20, and −40 °C. We tentatively assign the 0 °C endotherm to the first conformational change and a partial transition to the M phase. In this temperature regime the only major X-ray characteristics on slow cooling (not shown) are a monotonic shift and sharpening of the broad scattering peaks near 2θ angles of 7° and 15.2°. The second endotherm would then be associated with formation of the K_2 phase. Since there are no overt signatures of a backbone conformational change, the underlying impetus for this partial crystallization must arise from the influence of the alkyl side chains. Atactic poly(methyl-*n*-octadecylsilane) oligomers[41] also exhibit partial crystallization. The lowest temperature DSC feature, at −40 °C, therefore correlates with the second chain conformational change. In terms of the local structure, the formation of a T+D+T−D− dominated Si backbone can now be corroborated. There are no features in the conventional X-ray scattering which are suggestive of global changes in the interchain packing.

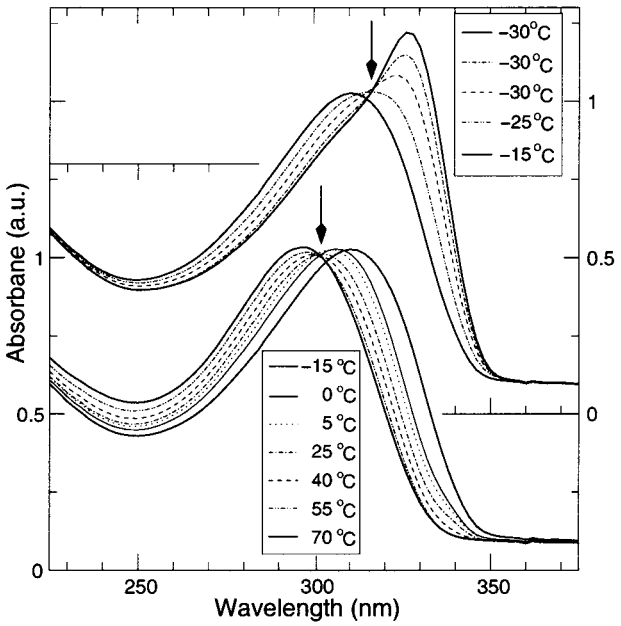

Figure 8. A series of UV absorption spectra for a pMeHexSi thin film during modest cooling (∼1 °C/min), demonstrating the existence of two distinct isosbestic points. The last two −30 °C spectra were taken 10 min apart and did not change thereafter.

We now revisit the claim[25] that the longer poly(methyl-*n*-alkylsilanes) are suitable for comparative studies in the context of Schweizer's[7,8] polarizable media theory because of the presumed amorphous nature of the polymer family at low temperatures. The work presented here demonstrates that, depending on the specific thermal history, partial crystallization of pMeHexSi does occur. Even though the presence of such transitions may invalidate direct comparisons to this theory, this does not appear to be the case for pMeHexSi. In both instances in which the pMeHexSi backbone conformation changed abruptly, there was no clear correlation to a gross phase change that profoundly altered the interchain packing. Hence, the crossover from a continuous to abrupt thermochromic transition on moving from pMeBuSi to pMeHexSi is still substantiated. However, the observed changes in the side chain packing do influence the process so that, in this case, three distinctly different conformational forms appear. This may well be the underlying explanation for the presence of two different low temperature conformational forms reported in recent solution studies of poly(di-*n*-hexylsilane).[42] Unfortunately, existing direct measurements of the local structure (in pMeHexSi), by PDF analysis, do not have sufficient sensitivity for resolving structural differences in the intermediate conformational state.

Conclusions

The highly asymmetric poly(methyl-*n*-alkylsilanes) exhibit a complex side chain length dependent behavior of nearly equal complexity to the more commonly studied symmetrically substituted systems. Partial crystallization on cooling appears to be a fairly common occurrence despite the atactic construction and this inherent disorder. Recent studies[43] of poly(methyl-*n*-dodecylsilane) also observe formation of an ordered structure on cooling. In retrospect the most surprising feature is that pMeBuSi does not form an ordered phase.

The underlying reason for this anomalous behavior is, as yet, unknown.

All three polymers reported here have typical values for their average Si−Si bond length (of 2.36 Å) and Si−Si−Si bond angle (of 116°). Beyond the nominal 4.00 Å Si second-nearest-neighbor spacing there are distinct temperature-dependent variations. The most planar form is consistent with a T+D+T−D− local construction. If either an AOAO′ or AGAG′structure is assumed, the next three Si neighbor distances become 5.35, 7.40, and 9.20 Å or 4.90, 7.10, and 8.65 Å, respectively. The shorter two of these repeats have been overlaid on the PDF data of Figure 6, and in no case are there simultaneously peaks at both AGAG′ positions even in the high-temperature data. On the other hand, all data sets which correspond to a more disordered phase (i.e., both pMeBuSi curves and pMeHexSi at 300 K) exhibit weak, but consistent, features at 5.35 and 7.40 Å which are appropriate for the AOAO′ conformer. Hence, there is some evidence for coexistence of the T+D+T−D− unit with a comparable A (or more likely T)/O-based motif. Comprehensive molecular dynamics simulations may be able to better resolve this claim.

In a more general setting it is clear that these polymers cannot always be viewed using the generic description that the observed thermochromism is simply representative of a two-phase transition between an ordered state at low temperature and a disordered one at high temperature. The molecular level competition between the distinctive ordering mechanisms for the backbone and side chains gives rise to considerable diversity.

Acknowledgment. We gratefully acknowledge support of this work through NSF Grants DMR-9810623 (R.W.) and DMR-0077698 (W.C. and M.J.W.). Support of the X7A beam line by Brookhaven National Laboratory (under the DOE) is also acknowledged. We also thank S. S. Bukalov and L. A. Leites for communication of their unpublished work.

References and Notes

(1) Miller, R. D.; Michl, J. *Chem. Rev.* **1989**, *89*, 1359.
(2) West, R. In *Comprehensive Organometallic Chemisty II*; Davies, A. G., Ed.; Pergamon: Oxford, 1994; Vol. 2, Chapter Organopolysilanes, p 77.
(3) Lacave-Goffin, B.; Hevesi, L.; Demoustier-Champange, S.; Devaux, J. *ACH−Models Chem.* **1999**, *136*, 214.
(4) Michl, J.; West, R. In *Silicon-Based Polymers: The Science and Technology of Their Synthesis and Applications*; Chojnowski, J., Jones, R. G., Ando, W., Eds.; Chapman and Hall: New York, 1999; Chapter Electronic Structure and Spectroscopy of Polysilanes, in press.
(5) Harrah, L. A.; Zeigler, J. M. *J. Polym. Sci., Polym. Lett. Ed.* **1985**, *23*, 209.
(6) Rabolt, J. F.; Hofer, D.; Miller, R. D.; Fickes, G. N. *Macromolecules* **1986**, *19*, 611.
(7) Schweizer, K. S. *J. Chem. Phys.* **1986**, *85*, 1156.
(8) Schweizer, K. S. *Synth. Met.* **1989**, *28*, C565.
(9) Kanai, T.; Ishibashi, H.; Hayashi, Y.; Ogawa, T.; Furukawa, S.; West, R.; Dohmaru, T.; Oka, K. *Chem. Lett.* **2000**, 650.
(10) Koe, J. R.; Fujiki, M.; Nakashima, H. *J. Am. Chem. Soc.* **1999**, *121*, 9734.
(11) Chunwchirasiri, W.; West, R.; Winokur, M. J. *Macromolecules* **2000**, *33*, 9720.
(12) Lovinger, A. J.; Davis, D. D.; Schilling, F. C.; Padden, F. J.; Bovey, F. A.; Zeigler, J. M. *Macromolecules* **1991**, *24*, 132.
(13) Karikari, E. K.; Greso, A. J.; Farmer, B. L.; Miller, R. D.; Rabolt, J. F. *Macromolecules* **1993**, *26*, 3937.
(14) Miller, R. D.; Farmer, B. L.; Fleming, W.; Sooriyakumaran, R.; Rabolt, J. F. *J. Am. Chem. Soc.* **1987**, *109*, 2059.
(15) Schilling, F. C.; Lovinger, A. J.; Zeigler, J. M.; Davis, D. D.; Bovey, F. A. *Macromolecules* **1989**, *22*, 3055.
(16) Mintmire, J. W. *Phys. Rev. B* **1989**, *39*, 13350.
(17) Tachibana, H.; Matsumoto, M.; Tokura, Y.; Moritomo, Y.; Yamaguchi, A.; Koshihara, S.; Miller, R. D.; Abe, S. *Phys. Rev. B* **1993**, *47*, 4363.
(18) Tersigni, S.; Ritter, P.; Welsh, W. J. *J. Inorg. Org. Polym.* **1991**, *1*, 377.
(19) Patnaik, S. S.; Farmer, B. L. *Polymer* **1992**, *33*, 5121.
(20) Neumann, F.; Teramae, H.; Downing, J. M.; Michl, J. *J. Am. Chem. Soc.* **1998**, *120*, 573.
(21) Albinsson, B.; Antic, D.; Neumann, F.; Michl, J. *J. Phys. Chem.* **1999**, *103*, 2184.
(22) Winokur, M. J.; Koe, J. R.; West, R. *Polym. Prepr.* **1997**, *38* (2), 57.
(23) Jambe, B.; Jonas, A.; Devaux, J. *J. Polym. Sci., Polym. Phys.* **1997**, *35*, 1533.
(24) Furukawa, S. *J. Organomet. Chem.* **2000**, *611*, 36.
(25) Yuan, C.-H.; West, R. *Macromolecules* **1994**, *27*, 629.
(26) Chunwachirasiri, W.; West, R.; Winokur, M. J. *Macromolecules* **2000**, *33*, 9720.
(27) Trefonas, P.; West, R.; Miller, R. D.; Hofer, D. *J. Polym. Sci., Polym. Lett. Ed.* **1983**, *21*, 819.
(28) Asuke, T.; West, R. *J. Inorg. Organomet. Polym.* **1995**, *5*, 31.
(29) Prosa, T. J.; Winokur, M. J.; Moulton, J.; Smith, P.; Heeger, A. J. *Macromolecules* **1992**, *25*, 4364.
(30) Narten, A. H. *J. Chem. Phys.* **1989**, *90*, 5857.
(31) Winokur, M. J. In *Local Structure from Diffraction*; Billinge, S. J. L., Thorpe, M. F., Eds.; Plenum Press: New York, 1998; p 337.
(32) Resel, R.; Leising, G.; Lunzer, F.; Marschner, C. *Polymer* **1998**, *39*, 5257.
(33) Winokur, M. J.; Mattes, B. R. *Phys. Rev. B* **1996**, *54*, R12637.
(34) Yokoyama, K.; Yokoyama, M. *Philos. Mag. B* **1990**, *61*, 59.
(35) Kato, H.; Sasanuma, Y.; Kaito, A.; Tanigaki, N.; Tanabe, Y.; Kinugasa, S. *Macromolecules* **2001**, *34*, 262.
(36) Although the displayed scale is terminated at 375 nm, the absorption curve remains featureless out beyond 400 nm.
(37) In some instances Bukalov and Leites (Bukalov, S. S.; Leites, L. A., unpublished results) have observed very weak shoulders extending out to 380 nm.
(38) MM2 force fields employed using modeling package MacroModel from Schrödinger, Inc.
(39) Modeling of all PDF data sets was undertaken, but the raw X-ray data included sample specific systematic artifacts which were difficult to isolate. These effects prevented a more quantitative analysis.
(40) Ge, J. J.; Zhang, A.; McCreight, K. W.; Ho, R. M.; Wang, S. Y.; Jin, X.; Harris, F. W.; Cheng, S. Z. D. *Macromolecules* **1999**, *30*, 66498.
(41) Wu, Z. M.; Xie, F. C.; Hu, Z. J.; Liu, J. P.; Du, B. Y.; He, T. B. *Polymer* **2000**, *42*, 1047.
(42) Bukalov, S. S.; Leites, L. A.; West, R., submitted to *Macromolecules*.
(43) Unpublished results.

MA0105688